# TRANSMISSION OF IMAGES USING MULTI-SCROLL AND MULTI-DIRECTION SNLF CHAOTIC SYSTEMS

## *TRANSMISIÓN DE IMÁGENES USANDO SISTEMAS CAÓTICOS SNLF MULTI-ENRROLLAMIENTO Y MULTI-DIRECCIÓN*

***José Cruz Núñez Pérez***
Instituto Politécnico Nacional
*nunez@citedi.mx*

***Vincent Ademola Adeyemi***
Instituto Politécnico Nacional
*vademola@citedi.mx*

***Francisco Javier Pérez Pinal***
Tecnológico Nacional de México en Celaya
*francisco.perez@itcelaya.edu.mx*

***Aldo Bonilla Rodríguez***
Instituto Politécnico Nacional
*aldo.bonilla.r@gmail.com*

***Gamaliel Entrambasaguas León***
Instituto Politécnico Nacional
*gamaliel.e.leon@gmail.com*

***Rodrigo Yaoctzin Serrato Andrade***
Instituto Politécnico Nacional
*serrato.yaoctzin@gmail.com*

***Andrés Calvillo Téllez***
Instituto Politécnico Nacional
*calvillo@citedi.mx*

## Abstract

This paper describes the procedure for the development of multi-scrolls and 1-2-3 directions chaotic systems, based on saturated nonlinear functions SNLF. Moreover, we explain how to design a system based on chaotic oscillators for encryption, transmission and decryption of messages which for this paper are RGB type. Finally, the encryption, transmission, and decryption processes were done through a graphical user interface developed on Matlab® software for an immediate application of the encryption techniques and SNLF chaotic algorithms.

**Keywords:** *Chaotic systems, Chua oscillator, Encryption, RGB image, SNLF.*

## Resumen

Este trabajo muestra el procedimiento para el desarrollo de un sistema caótico de multi-enrollamientos en 1-2-3 direcciones, basado en funciones no lineales saturadas SNLF. Además, se explica cómo diseñar un sistema basado en dichos osciladores para la encriptación, transmisión y decodificación de mensajes, que para este artículo son imágenes RGB. Finalmente, los procesos de encriptación, transmisión y decodificación de las imágenes fueron hechos a través de una interfaz gráfica de usuario desarrollada en el software Matlab® que le permite al usuario aplicar de manera inmediata las técnicas de encriptación usando algoritmos caóticos de SNLF.

**Palabras Claves:** Encriptación, imagen RGB, SNLF, Oscilador de Chua, Sistemas caóticos.

## 1. Introduction

The study of chaos has been of great interest to researchers in the last few decades perhaps due to its potential applications. The concept of chaos was first studied by Henri Poincaré, a French mathematician between 1887 and 1890. He was the first to point out that many deterministic systems display a sensitive dependence on initial conditions. It is noteworthy to state that the study of chaos was actually an unexpected discovery born from a mistake Poincaré made while solving the infamous “three-body problem”. He stated that small differences (i.e. error) in the initial conditions of a deterministic system lead to very great differences in the final phenomena.

However, it was not until 1963 that the term chaos theory was coined by Edward Lorenz, a meteorologist. It is interesting to note also that his discovery of chaos was also accidental. Chaos theory, also known as the “Butterfly Effect” in 1972, became a subject of research ever since.

The study of chaos has shown that the phenomenon has three major properties, namely oscillating (aperiodic) movements, deterministic and sensitivity to initial

conditions [Sprott, 2003]. Chaos has oscillating movements because the trajectories do not fit a fixed point, periodic orbit or quasi-periodic orbit. It is deterministic because the system is not random. The irregular behaviour of chaotic system is as a result of its inherent nonlinearity. Chaos is sensitive to initial conditions because very similar initial conditions produce different behaviours in the trajectories after a long enough time. That is, trajectories beginning with very close initial conditions eventually separate exponentially. This particular property makes long-term prediction of chaos impossible.

Chaos has applications in several disciplines including telecommunications [Tlelo-Cuautle, e*t al.*,2015, Maldonado and Hernandez, 2007] in which secure information transmission is of great importance. In this work, chaotic systems of SNLF type were simulated and employed to encrypt, transmit and receive RGB images.

## 2. Methods

### Non-linear Saturated Functions

A chaotic oscillator based on saturated nonlinear functions SNLF can be described by the following system of differential equations 1 [Tlelo-Cuautle, *et al.*, 2013].

$$\begin{aligned} \frac{dx}{dt} &= y \\ \frac{dy}{dt} &= z \\ \frac{dz}{dt} &= -ax - by - cz + d_1 f(x; k, \alpha, h, p, q) \end{aligned} \tag{1}$$

Where $a$, $b$, $c$ and $d_1$ are proposed positive real coefficients, with values in the interval [0 1]. Zero initial conditions for x, y and z are also required due to the interdependence of the state variables.

The system has a non-linear dynamic behaviour, thanks to the saturated destabilizing function $f$ ($x$; $k$; $\propto$,, $h$, $p$, $q$). The purpose of this function is to provide feedback to the system and keep it oscillating without the need for an extra input variable in the system. In addition, chaotic behaviour in the system is ascribed to

the destabilizing function. The saturated nonlinear function can be described by a piecewise linear (PWL) function whose shape depends on the number of scrolls required in the chaotic system [Munoz-Pacheco *et al*, 2012]. The PWL approximation of the SNLF is given by equation 2.

$$f(x;k,\propto,h,p,q) = \sum_{i=-p}^{q} f_i\,(x;k,\propto,h) \tag{2}$$

Where $k,\propto and\ h$ are parameters to describe the PWL segments, and $p,q$ are used to evaluate the number of scrolls.

**Chaotic Oscillator of Chua**

The Chua diode can generate an *"n"* number of scrolls in a dynamic system due to its non-linear negative resistance behaviour. The system mentioned above can be seen in figure 1 [Obeso-Rodelo, 2015].

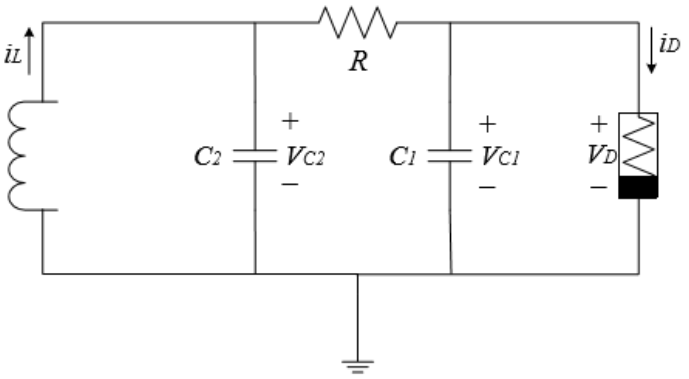


Figure 1 Circuit based on the Chua diode.

From the previous circuit the differential equations that describe their behaviour can be obtained by applying the laws of Kirchhoff [Sánchez- Lopez, *et al.*, 2011], being expressed as in equation 3.

$$C_1\frac{dV_{c_1}}{dt} = G\left(V_{C_2} - V_{C_1}\right) - g(V_{C_1})$$
$$C_2\frac{dV_{c_2}}{dt} = G\left(V_{C_1} - V_{C_2}\right) + i_L) \tag{3}$$

$$L\frac{di_L}{dt} = -V_{C_2}$$

Where $G = \frac{1}{R}$, $V_{C_1}$, $V_{C_2}$, and $i_L$ are respectively the voltages in the capacitor $C_1$, $C_2$ and the current in the inductor. In addition, for the function that grants non-linearity to the system, the function of the Chua diode is defined as equation 4.

$$g(V_{C_1}) = G_P V_{C_1} + \frac{1}{2}(G_A - G_P)\left[|V_{C_1} + P| - |V_{C_1} - P|\right]\frac{dy}{d\tau} = x - y + z \qquad (4)$$

The system of differential equations above can be transported to a normalized dimensionless form. The above is achieved by making the following changes of variables $x = \frac{V_{C_1}}{P}, y = \frac{V_{C_2}}{P}, z = \frac{i_L}{PG}, \tau = \frac{tC_2}{G}$ . And taking into account that $\alpha = \frac{C_2}{C_1}$, $\beta = \frac{C_2}{LG_2}$, $m_0 = RG_A$ and $m_1 = RG_P$, the equation 5 is given.

$$\frac{dx}{d\tau} = \alpha[y - x - g(x)]$$

$$\frac{dy}{d\tau} = x - y + z$$

$$\frac{dz}{d\tau} = -\beta y$$

$$g(x) = m_1 x + \frac{1}{2}(m_0 - m_1)[|x+1| - |x-1|] \qquad (5)$$

As stated above, the function *g(x)* is responsible for the non-linear behaviour of the Chua diode [Elhadj and Sprott, 2010; Yang and Chua, 2000; Guerra, *et al.*, 2010].

**Multi-Direction Oscillators**

Chaotic oscillators can increase, in addition to the number of scrolls, the directions of growth. To achieve this it is necessary to carry out the following mathematical relations [Lü and Chen, 2017; Lü, *et al.,* 2008] in equations 6–9.

$$\dot{X} = BX + B\varphi(CX) \qquad (6)$$

$$X = (x, y, z)^T \qquad (7)$$

$$A = \begin{pmatrix} 0 & 1 & 0 \\ 0 & 0 & 1 \\ -a & -b & -c \end{pmatrix} \quad (8)$$

$$A = \begin{pmatrix} 0 & -d2/b & 0 \\ 0 & 0 & -d3/c \\ d1 & d2 & d3 \end{pmatrix} \quad (9)$$

and *C* is the identity matrix.

Equation 6 is a general expression for the development of chaotic oscillators in 1-2-3 directions, while the equations 7, 8 and 9 are specific descriptions for the system of equations 1.

The matrix ***φ(CX)*** represents the set of non-linear saturated functions generating scrolls in 1, 2 and 3 directions as represented in equations 10, 11 and 12, respectively [Lü and Chen, 2017].

$$\varphi(CX) = \begin{pmatrix} f(x; k_1, \alpha, h_1, p_1, q_1) \\ 0 \\ 0 \end{pmatrix} \quad (10)$$

$$\varphi(CX) = \begin{pmatrix} f(x; k_1, \alpha, h_1, p_1, q_1) \\ f(y; k_2, \alpha, h_2, p_2, q_2) \\ 0 \end{pmatrix} \quad (11)$$

$$\varphi(CX) = \begin{pmatrix} f(x; k_1, \alpha, h_1, p_1, q_1) \\ f(y; k_2, \alpha, h_2, p_2, q_2) \\ f(z; k_3, \alpha, h_3, p_3, q_3) \end{pmatrix} \quad (12)$$

**Synchronization of Chaotic Oscillators of the SNLF Type**

In this work, synchronization of SNLF oscillators was performed by state observers. During synchronization by observers, the first system, the master, is to which the state variables of the second system, the slave, will approximate. The latter will take the observer of states.

The master system must be expressed mathematically such that it can adapt to the observer of slave system states. Due to the above reason, both systems are expressed in their Generalized Hamiltonian canonical form [Sánchez-Lopez *et al*, 2011; Carbajal-Gómez, 2015], thus fulfilling the expression in equation 13.

$$\dot{x} = \mathcal{J}(x)\frac{\partial \mathrm{H}}{\partial x} + \mathcal{S}(x)\frac{\partial \mathrm{H}}{\partial x} + \mathcal{F}(x) \tag{13}$$

Where the matrices $\mathrm{H}(\mathrm{x})$, $\mathcal{J}(\mathrm{x})$ y $\mathcal{S}(\mathrm{x})$ in equations 14, 15 and 16 respectively.

$$\frac{\partial \mathrm{H}}{\partial x} = \mathrm{M\,x} \tag{14}$$

$$\mathcal{J}(x) + \mathcal{J}^{\mathrm{T}}(x) = 0 \tag{15}$$

$$\mathcal{S}(x) = \mathcal{S}^{T}(x) \tag{16}$$

In addition, $\mathcal{F}(\mathrm{x})$ represents the destabilizing function of the system, which in this case is the SNLF function. In order to carry out the observer, it is necessary to give an exit to the system. The system is shown in equation 17.

$$y = \mathcal{C}\frac{\partial \mathrm{H}}{\partial x} \tag{17}$$

Where $\mathcal{C}$ is a proposed matrix.

Once the master system is defined, the same is done with the slave system. However, in the latter one must add the error together with the observer's profits, leaving the expressions in equations 18 and 19.

$$\dot{\xi} = \mathcal{J}(\xi)\frac{\partial \mathrm{H}}{\partial \xi} + \mathcal{S}(\xi)\frac{\partial \mathrm{H}}{\partial \xi} + \mathcal{F}(\xi) + \mathcal{K}e \tag{18}$$

$$\eta = \mathcal{C}\frac{\partial H}{\partial \xi} \tag{19}$$

$\mathcal{K}$ being the gain of the observer and $e$ the error that is given by the following expression in equation 20.

$$e = y - \eta \tag{20}$$

The above expressions are applied to the system of equations 1 and, according to the proposed matrix $\mathcal{C}$, different observers can be obtained. For this work, observers were made with two different state variables. The variable $x$ was used

for the increasing oscillators in one and three directions and $y$ for the increasing oscillator in two directions.

For the oscillator increasing in one direction, the expressions are given in equations 21 and 22.

$$\begin{aligned} \dot{x}_1 &= x_2 \\ \dot{x}_2 &= x_3 \\ \dot{x}_3 &= -ax_1 - bx_2 - cx_3 + d_1 f(x_1; k, \alpha, h, p, q) \end{aligned} \tag{21}$$

$$\begin{aligned} \dot{y}_1 &= y_2 + k_1(x_1 - y_1) \\ \dot{y}_2 &= y_3 + k_2(x_1 - y_1) \\ \dot{y}_3 &= -ay_1 - by_2 - cy_3 + d_1 f(x_1; k, \alpha, h, p, q) + k_3(x_1 - y_1) \end{aligned} \tag{22}$$

For the oscillator increasing in two directions, the expressions are given in equations 23 and 24.

$$\begin{aligned} \dot{x}_1 &= x_2 - \frac{d_2}{b} f(x_2; k, \alpha, h, p, q) \\ \dot{x}_2 &= x_3 \\ \dot{x}_3 &= -ax_1 - bx_2 - cx_3 + d_1 f(x_1; k, \alpha, h, p, q) + d_2 f(x_2; k, \alpha, h, p, q) \end{aligned} \tag{23}$$

$$\begin{aligned} \dot{y}_1 &= y_2 - \frac{d_2}{b} f(x_2; k, \alpha, h, p, q) + k_1(x_2 - y_2) \\ \dot{y}_2 &= y_3 + k_2(x_2 - y_2) \\ \dot{y}_3 &= -ay_1 - by_2 - cy_3 + d_1 f(x_1; k, \alpha, h, p, q) + d_2 f(x_2; k, \alpha, h, p, q) + k_3(x_2 - y_2) \end{aligned} \tag{24}$$

For the oscillator increasing in three directions, the expressions are given in equations 25 and 26.

$$\begin{aligned} \dot{x}_1 &= x_2 - \frac{d_2}{b} f(x_2; k, \alpha, h, p, q) \\ \dot{x}_2 &= x_3 - \frac{d_3}{c} f(x_3; k, \alpha, h, p, q) \\ \dot{x}_3 &= -ax_1 - bx_2 - cx_3 + d_1 f(x_1; k, \alpha, h, p, q) + d_2 f(x_2; k, \alpha, h, p, q) \\ &\quad + d_3 f(x_3; k, \alpha, h, p, q) \end{aligned} \tag{25}$$

$$\dot{y}_1 = y_2 - \frac{d_2}{b} f(x_2; k, \alpha, h, p, q) + k_1(x_1 - y_1)$$

$$\dot{y}_2 = y_3 - \frac{d_3}{c} f(x_3; k, \alpha, h, p, q) + k_2(x_1 - y_1) \tag{26}$$

$$\dot{y}_3 = -ay_1 - by_2 - cy_3 + d_1 f(x_1; k, \alpha, h, p, q) + d_2 f(x_2; k, \alpha, h, p, q) + d_3 f(x_3; k, \alpha, h, p, q) + k_3(x_1 - y_1)$$

**Encryption of Information with Chaotic Oscillators**

With the synchronization of chaotic systems it is possible to create a secure data transmission system [Sánchez-Lopez, *et al.*, 2011]. In this work, this system was made taking as an advantage the error induced between the state variables in the systems. Given that the slave system follows the master system in its behaviour, the state variables do not present any variation so that it is possible, after a while, to induce an error. This induced error represents the information to be encrypted.

Working with observers requires that a specific state variable be used to correct the error, leaving two variables available for the encryption of the information. Before continuing the explanation with each system independently, it is necessary to clarify what was the sequence followed for the encryption, sending and decryption of information in all systems.

First, the master and slave systems were executed until a maximum error of 0.0000001 was obtained, which is enough to declare both systems synchronized. Once the synchronization is achieved, each determined number of points is sent a data of the information to be encrypted to the master system. The master system automatically recognizes the amount of time that must be executed according to the size of the image. In each of these points a state variable is injected with a byte of information of the image to be transmitted. Because the systems are synchronized, the slave system receives from the master system the signal of the state variable that has the encrypted signal. Despite this, the slave system still receives the error correction signal. Taking into account that this must be less than 0.0000001, the master-slave system must be able to recognize a large error by subtracting the state variables that contain the encrypted signal.

For the system with chaotic oscillators increasing in one direction, the variable $x_3$ was used as the encryption variable, so that the master system sends only the variables $x_1$ and $x_3$ to synchronize the systems and encrypt the image, respectively. In the system with chaotic oscillators increasing in two directions, the variables $x_2$ and $x_1$ were used to synchronize the systems and encrypt the information, respectively. In the case of the system with chaotic oscillators increasing in three directions, the variables $x_1$ and $x_2$ were used to synchronize the systems and encrypt the information, respectively. A graphical user interface was made in Matlab® with the purpose of simulating the synchronization of the systems and the encryption of the information to be transmitted. The interface allows you to select the type of oscillator and the image you want to transmit.

## 3. Results

Chaotic oscillator of the SNLF type were used to generate multi-scrolls in multi-directions. For example, figures 2 shows chaotic oscillator of the SNLF type in a) one, b) two and b) three directions, respectively. All oscillators have ten (10) scrolls in the proposed directions.

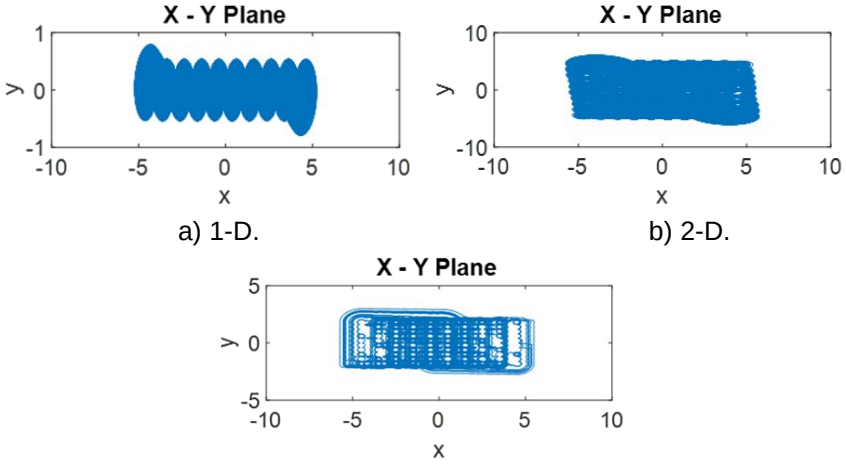


a) 1-D. b) 2-D.

c) 3-D.

Figure 2 Chaotic oscillator SNLF of 10 scrolls.

For all systems, a saturation of 300 units and an integration step of 0.1 was established. In addition, all physical parameters were assigned a value of 0.7. For

the system 21, these initial conditions were used: $x_1(0) = 0$, $x_2(0) = 0$ and $x_3(0) = 0.1$.

For the system of differential equations 22, which is the slave system of system (21), these initial conditions were used: $y_1(0) = 1$, $y_2(0) = -0.5$ and $y_3(0) = 3$. The observer gains used were $k_1 = 2$, $k_1 = 2$ and $k_3 = 7$.

In order to not saturate the computer system used, only the results obtained for oscillators of 10 scrolls increasing in one direction will be shown. For the phase spaces of the systems 21 and 22, figure 3 was obtained.

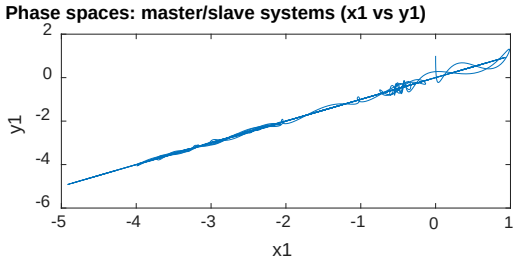


a) ($x_1$ vs $y_1$).

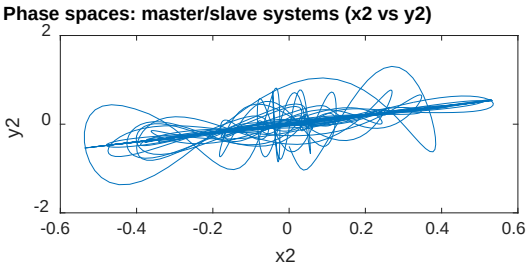


b) ($x_2$ vs $y_2$).

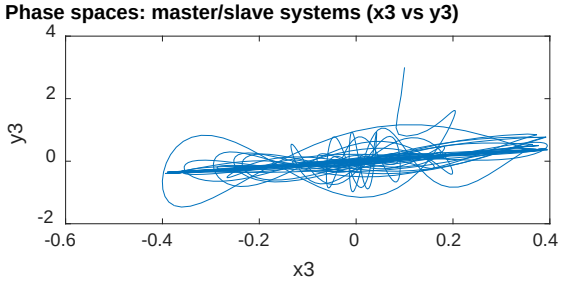


c) (x3 vs y3).

Figure 3 Phase space with 10 scrolls.

As one can see, the system has irregularities for a long time of iterations. This is due to the separation between initial conditions and the time in which the state

observer achieves synchronization. In figure 4 one can see the error between the master and slave systems for each state variable, as well as the number of integrations needed to achieve synchronization.

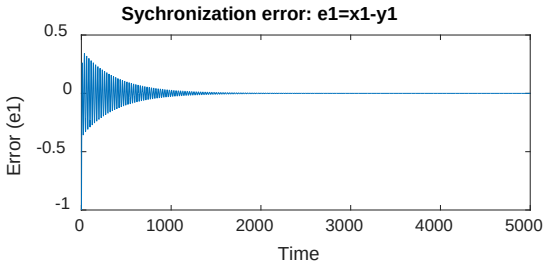


a) ($e_1=x_1-y_1$).

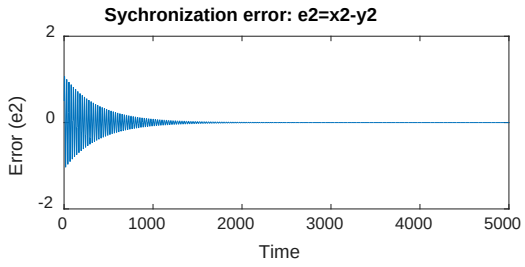


b) ($e_2=x_2-y_2$).

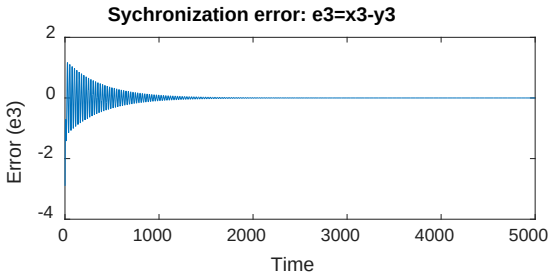


c) ($e_3=x_3-y_3$).

Figure 4 Error between systems with 10 scrolls in 1-D.

The systems seem synchronized from the 2.200 integration. However, the computer does not consider a complete synchronization until the error is less than 0.0000001. Taking into account this, it was until the 4.352nd iteration that the computer took as the synchronization of the master-slave systems.

For the case of the oscillator increasing in two directions, the system of differential equations 23 was used applying the initial conditions: $x_1(0) = 0.5$, $x_2(0) = 1$ and $x_3(0) = 0.7$.

For the slave system of equation 23, which is described by means of the differential equations 24, the initial conditions $y_1(0) = 0.1$, $y_2(0) = 0.2$ $y_3(0) = 0.4$ and were used, as well as the observer gains $k_1 = 0$, $k_2 = 0$ and $k_3 = 2$.

Only the results obtained from the synchronization of a master-slave system of 20 scrolls in 2 directions will be presented, figure 5 shows the phase states.

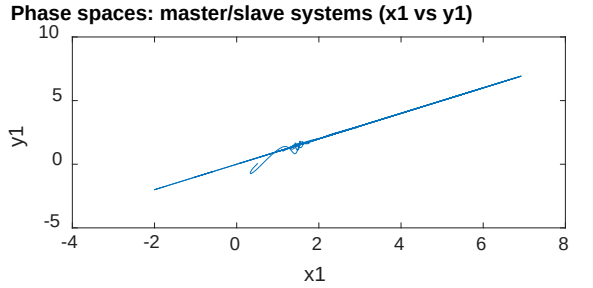


a) ($x_1$ vs $y_1$).

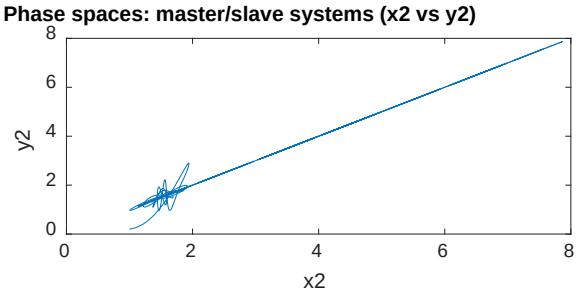


b) ($x_2$ vs $y_2$).

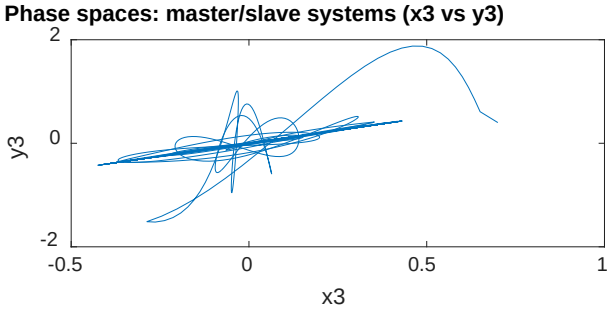


c) ($x_3$ vs $y_3$).

Figure 5 Phase space with 20 scrolls in 2-D.

As can be seen, the system has certain irregularities for a long time of iterations. This is due to the separation between initial conditions and the time in which the observer achieves synchronization. Errors between systems are shown in figure 6.

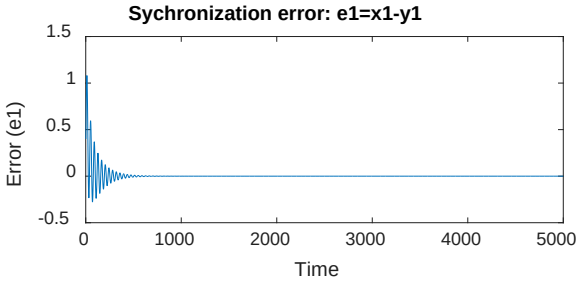


*a) ($e_1$=$x_1$-$y_1$).*

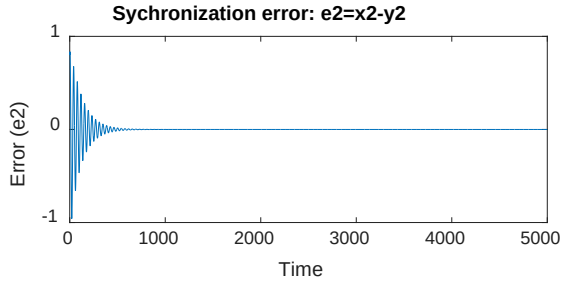


*b) ($e_2$=$x_2$-$y_2$).*

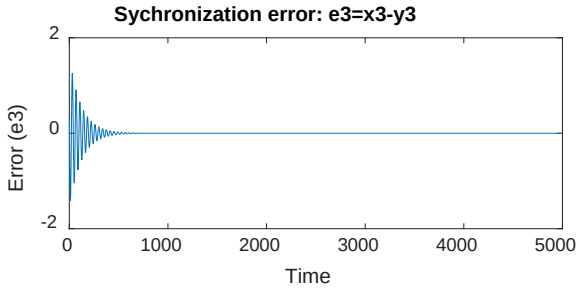


c) ($e_3$=$x_3$-$y_3$).

Figure 6 Error between systems with 20 scrolls in 2-D.

For this case, it takes about 736 iterations to stabilize both systems. Applying the same criterion of an error less than 0.0000001, it is after the 1,481th iterations that the computer considers synchronized to the master-slave system.

In the case of the differential equation systems 25 and 26, which represent the master and slave systems respectively, the initial conditions $x_1(0) = 0.5$, $x_2(0) = 1$ $x_3(0) = 0.7$, $y_1(0) = 0.1$, $y_2(0) = 0.2$ and $y_3(0) = 0.4$ were used. The profits of the observer of the system (26) are $k_1 = 2.3$, $k_2 = 0.1$ and $k_3 = 0.1$. To finish with the results as far as synchronization is concerned, the graphs obtained from the system with increasing oscillators in three directions and with 50 scrolls will be shown. The graphs of the phase states are presented in figure 7.

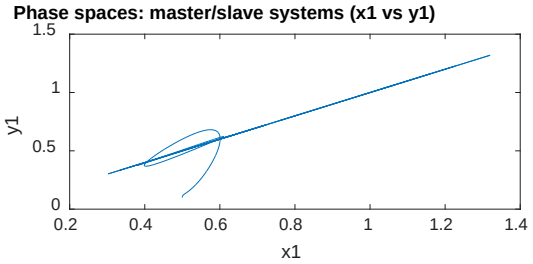


a) ($x_1$ vs $y_1$).

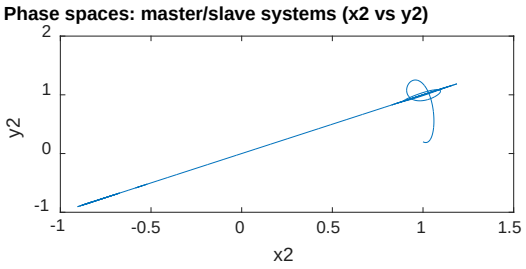


b) ($x_2$ vs $y_2$).

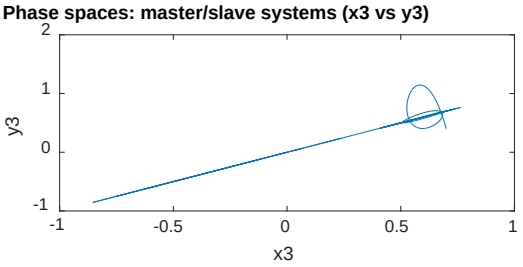


c) ($x_3$ vs $y_3$).

Figure 7 Phase space with 50 scrolls in 3-D.

It can be seen that the system does not present many variations, suggesting that the system takes less time to synchronize. Figures 8 confirms that the synchronization time is actually shorter.

Figures 8 demonstrates what was stated above, since the error does not exceed the unit, making the system stable, managing to be around only 1,994 iterations. However, the computer does not establish a complete synchronization until 2,090 iterations. The tests carried out in the systems suggested that they had a fast convergence to the master system using the variable $x_1$ in any case, but the behaviours in the variables $x_2$ and $x_3$ do not present behaviour as erratic as that seen in $x_1$. That is why it was decided to try to synchronize the systems with the variable $x_1$, leaving the safety level as a priority to speed. However, in the case of

the oscillator increasing in 2 dimensions it was not possible to do the synchronization using the variable $x_1$; it is for this reason that it was decided to use the variable $x_2$.

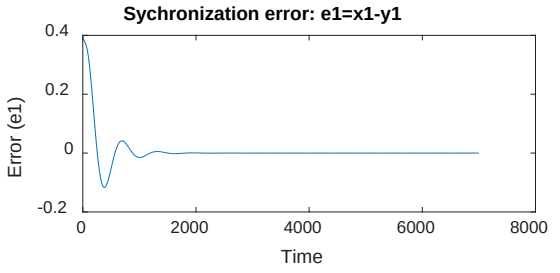


a) ($e_1=x_1-y_1$).

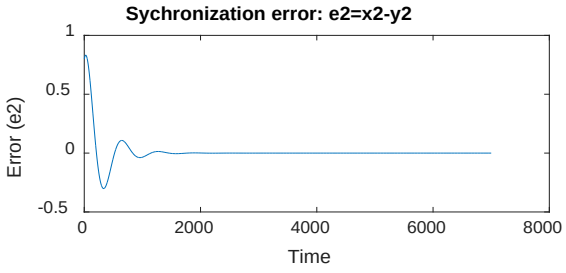


b) ($e_2=x_2-y_2$).

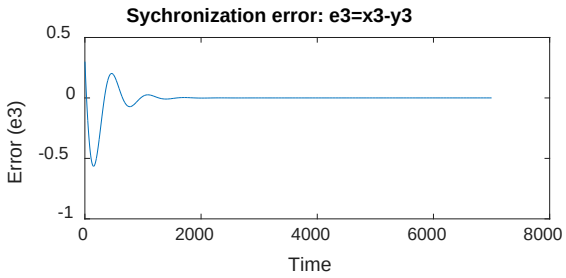


c) ($e_3=x_3-y_3$).

Figure 8 Error between systems with 50 scrolls in 3-D.

Thanks to the proposed saturation of 300 units, oscillators acquire values ranging between 500 and -500 units. The above allows the injection of the image bytes without any scaling, since the RGB values of each pixel in the image are within the closed interval [0 255]. Thanks to the above, the quality of the image to be transmitted is not modified in any way.

The image was sent byte by byte, and layer by layer, until the encryption, transmission and decryption were completed.

The results shown by the interface in Matlab® for transmitting a 271x186 RGB image in the three cases are contained in figures 9-11.

The correlation value permits to evaluate the close relationship between two images. The equation to compute the correlation coefficient is given in equation 27.

$$r = \frac{\sum_m \sum_n (A_{mn} - \overline{A})(B_{mn} - \overline{B})}{\sqrt{(\sum_m \sum_n (A_{mn} - \overline{A})^2)(\sum_m \sum_n (B_{mn} - \overline{B})^2)}} \quad (27)$$

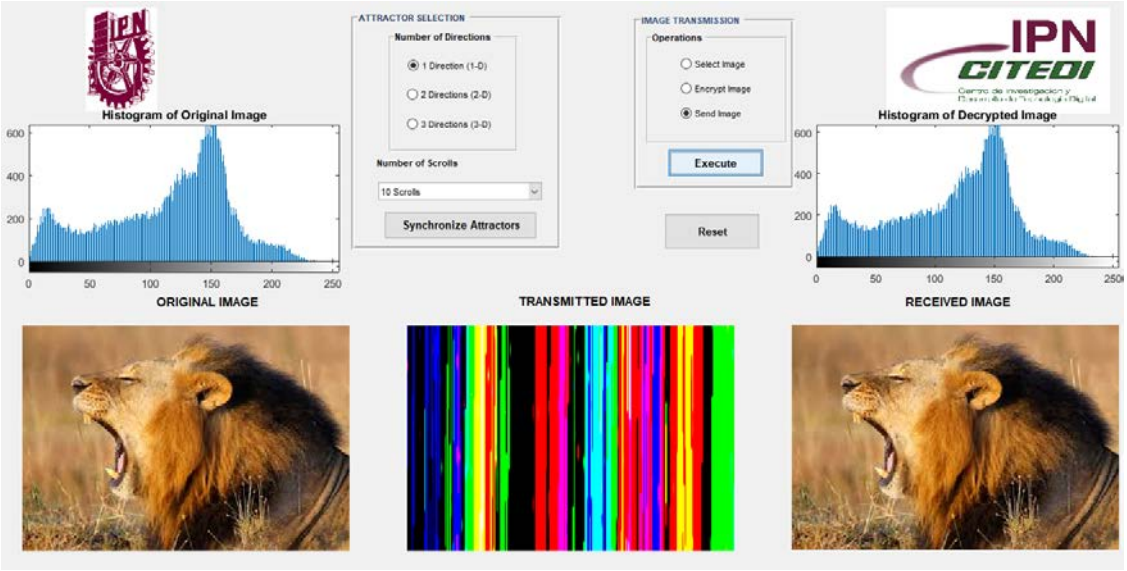


Figure 9 Transmission of image with 10 scrolls in 1-D.

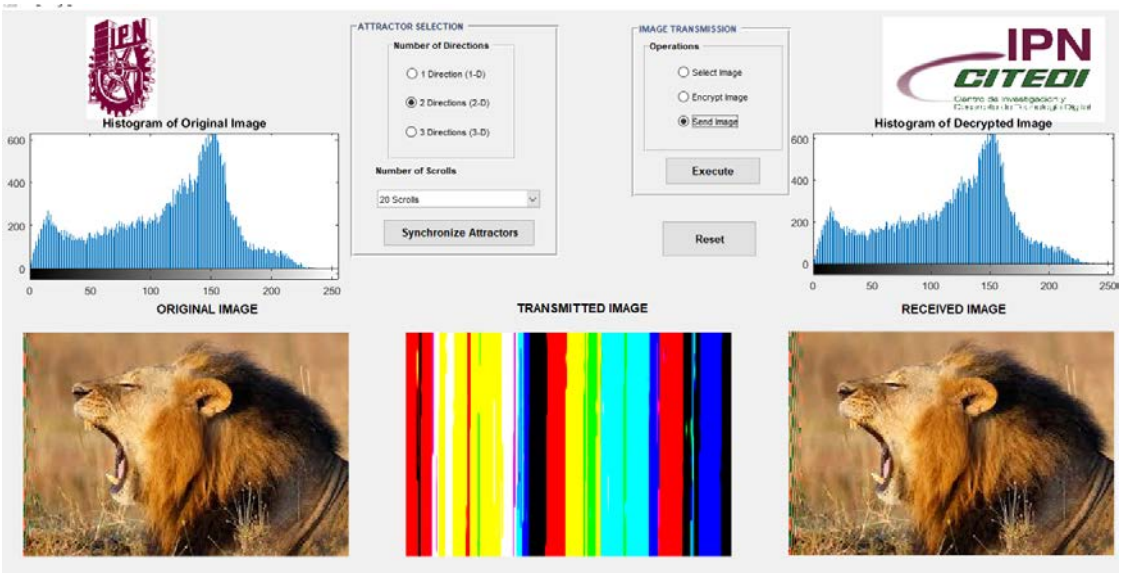


Figure 10 Transmission of image with 20 scrolls in 2-D.

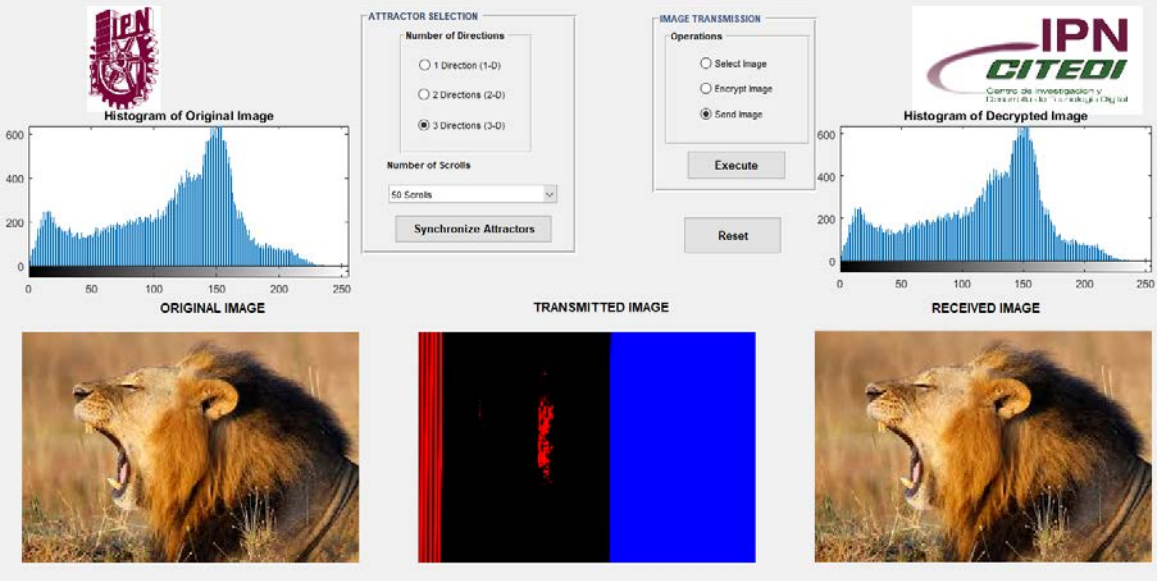


Figure 11 Transmission of image with 50 scrolls in 3-D.

The metrics shown in table 1 gives the correlation value between the original image and the encrypted image as well as the received image.

Table 1 Correlation Coefficients.

| Oscillator | Correlation Value | |
|---|---|---|
| | Encrypted Image | Received Image |
| 10 Scrolls 1-D | 0.0214 | 1 |
| 10 Scrolls 2-D | 0.0162 | 1 |
| 20 Scrolls 2-D | 0.0118 | 1 |
| 20 Scrolls 3-D | 0.0018 | 1 |
| 50 Scrolls 3-D | 0.0005 | 1 |

## 4. Discussion

As can be seen in table 1, when the system increases the number of scrolls and directions, the correlation between the encrypted signal and the original is decreasing [Obeso-Rodelo, 2015]. When deciphering the information, the system is able to obtain the image again virtually intact. This is the result of a strict criterion in the synchronization of the systems. It should also be mentioned that the system with fifty scrolls in three directions (figure 11), is more secured than the system with twenty scrolls in two directions (figure 10), which in turn is more secured than the system with ten scrolls in one direction (figure 9). This indicates that it is better to

opt for the growth in directions to the growth in scrolls. Finally, these parameters are directly related to the saturation given in the system.

Compared to other non-chaotic techniques [AL-Laham, 2015; Abdul Jaleel and Thomas, 2013; Wang X., Pei Q. and Li, 2014], the image transmission technique proposed in this work is less susceptible to interception because chaotic signals are known to be insensitive to initial conditions. Also, chaotic signals have a noise-like time series which makes transmission harder to detect by hackers when implemented in a physical transmission system. In addition, different chaotic systems can be implemented in this technique to achieve more robustness.

## 5. Conclusions

In this work, a methodology for encrypting, transmitting and decrypting a RGB image using SNLF chaotic systems was proposed. The systems utilized multi-scrolls in 1, 2 and 3 directions. Statistical analysis was carried out to show the confidentiality of the transmitted image. The results suggest that the systems present a fast synchronization using the first variable of the system as a synchronization variable, although this leaves the system with less security. In spite of this, the systems can compensate in this aspect if the saturation of the system is increased. The security of the system increases as the directions and scrolls do. However, it is always better to opt for growth in directions, since this presents an even more erratic behaviour in all state variables, compared to the growth of scrolls.

## 6. Bibliography and References

[1] Abdul Jaleel J. and Thomas J.M. Guarding Images using a Symmetric key Cryptographic Technique: Blowfish Algorithm. International Journal of Engineering and Innovative Technology, Vol. 3, No. 2, pp. 196–201, 2013.

[2] AL-Laham M. M. Encryption-Decryption RGB Color Image Using Matrix Multiplication. International Journal of Computer Science & Information Technology, Vol 7, No 5, pp. 109-119, 2015.

[3] Sprott J. C. Chaos and Time-series Analysis. Oxford University Press, pp. 10-11, 2003.

[4] Carbajal-Gómez V.H. Synchronization of Chaotic Oscillators Optimized by Applying Evolutionary Algorithms. Ph.D. Disertación, Instituto Nacional de Física, Óptica y Electrónica, 2015.

[5] Elhadj Z. and Sprott J.C. Generating 3-Scroll Attractors from one Chua Circuit. International Journal of Bifurcation and Chaos, Vol. 20, No. 1, pp. 135-144, 2010.

[6] Lü J. and Chen G. A. Brief Overview of Multi-Scroll Chaotic Attractors Generation. IEEE International Symposium on Circuits and Systems, pp. 702-705, 2006.

[7] Lü J., Murali K., Sinha S., Leung H. and Aziz-Alaoui M.A. Generating multi-scroll chaotic attractors by thresholding. Physics Letters A, Vol. 372, Issue 18, pp. 3234-3239, 2008.

[8] Maldonado J.A. and Hernandez J.A. Chaos theory applied to communications--part I: Chaos generators. Proceedings of the Electronics, Robotics and Automotive Mechanics Conference, pp. 50-55, 2007.

[9] Munoz-Pacheco J.M., Campos-López W., Tlelo-Cuautle E. and Sánchez López C. OpAmp, CFOA and OTA-Based Configurations to Design Multi-Scroll Chaotic Oscillators. Trends in Applied Sciences Research, Vol. 7, Issue 2, pp. 168-174, 2012.

[10] Obeso-Rodelo P.J. Diseño e implementación en un FPGA de oscilador caótico para aplicaciones en sistemas de seguridad. M.Sc. Disertación, CITEDI., Instituto Politécnico Nacional, Tijuana B.C., 2015.

[11] Sánchez-López C., Muñoz-Pacheco J.M., Carbajal-Gómez V.H., Rodolfo-Trejo G., Ramírez-Soto C., Echeverria-Solis O.S. and Tlelo-Cuautle E. Design and Applications of Continuous-Time Chaos Generators. Book: Chaotic Systems, IntechOpen, pp. 227-254, 310 pages, February 2011.

[12] Yang T. and Chua L.O. Piecewise-linear Chaotic Systems with a Single Equilibrium Point. International Journal of Bifurcation and Chaos, Vol. 10, Issue. 9, pp. 2015-2060, 2000.

[13] Tlelo-Cuautle E., Rodríguez D. G. H., Santillán J. H., Arreola V. H. and Cantera L. A. C. Simulation and Experimental Realization of Multi-Scroll

Chaotic Oscillators. Journal of Engineering Science and Technology, Review 6 (4), pp. 1-8, 2013.

[14] Tlelo-Cuautle E., Carbajal-Gomez V. H., Obeso-Rodelo P. J., Rangel-Magdaleno J. J. and Núñez-Pérez J. C. FPGA realization of a chaotic communication system applied to image processing. Nonlinear Dynamics Vol. 82, Issue 4, pp. 1879-1892, 2015.

[15] Trejo-Guerra R., Tlelo-Cuautle E., Sanchez-López C., Munoz-Pacheco J. M., and Hernández Cruz C. Realization of multiscroll chaotic attractors by using current-feedback operational amplifiers. Revista Mexicana de Física Vol. 56, Issue 4, pp. 268–274, 2010.

[16] Wang X., Pei Q. and Li H. A Lossless Tagged Visual Cryptography Scheme. IEEE Signal Processing Letters, Vol. 21, No. 7, pp. 853–856, 2014.